

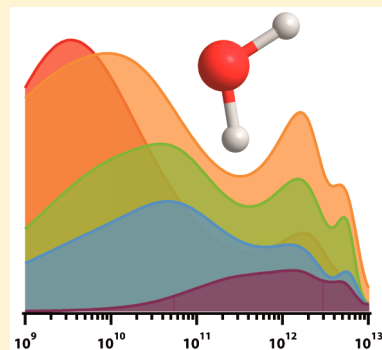
Spectrum of Slow and Super-Slow (Picosecond to Nanosecond) Water Dynamics around Organic and Biological Solutes

Gopakumar Ramakrishnan, Mario González-Jiménez,^{1b} Adrian J. Laphorn, and Klaas Wynne^{*1b}

School of Chemistry, WestCHEM, University of Glasgow, Glasgow G12 8QQ, United Kingdom

 Supporting Information

ABSTRACT: Water dynamics in the solvation shell of solutes plays a very important role in the interaction of biomolecules and in chemical reaction dynamics. However, a selective spectroscopic study of the solvation shell is difficult because of the interference of the solute dynamics. Here we report on the observation of heavily slowed down water dynamics in the solvation shell of different solutes by measuring the low-frequency spectrum of solvation water, free from the contribution of the solute. A slowdown factor of ~ 50 is observed even for relatively low concentrations of the solute. We go on to show that the effect can be generalized to different solutes including proteins.



Solvation of molecules, in particular by water, is of great importance for the understanding of (bio)chemical reactivity and the determination of solubilities and biological interactions vital to living organisms.¹ For example, in the case of DNA and proteins, the hydration layer is essential in determining conformation and function.² The wide range in the relaxation times of water in the solvation shell predicted by theoretical modeling was only recently experimentally observed in DNA.^{3,4} However, no experimental technique has yet allowed a detailed description of the distribution of relaxation time scales.

The diffusive orientational and translational motions of liquid water, as well as the hydrogen-bond bend and stretch modes, are in the gigahertz to terahertz frequency range and have been widely studied using dielectric relaxation spectroscopy,^{5–7} far-infrared and terahertz time-domain spectroscopy (THz-TDS),⁸ and Raman and optical Kerr-effect techniques.^{9–11} On adding solutes, the dynamics of water in the solvation shell is expected to change to a greater or lesser extent, giving rise to changes in the low-frequency spectrum. However, diffusive and librational motions of the solute itself tend to mask these changes considerably.^{12–14}

We have applied the technique of ultrafast optical Kerr-effect (OKE) spectroscopy, which measures the depolarized Raman spectrum using a time-domain technique.¹⁵ The OKE setup and data analysis are discussed in detail in the [Supporting Information \(SI\)](#). OKE measures the correlation function of the anisotropic polarizability tensor and is therefore sensitive to reorientational molecular motions.¹⁶ Thus this provides an opportunity to “switch-off” signals by using appropriately chosen solutes or solvents to isolate certain physical effects. For example, we have used this idea in studying noble-gas liquids¹⁷ in which the OKE signal can only come from collision-induced effects. It was also applied in concentrated aqueous solutions of

simple inorganic salts^{11,18} where high concentrations were shown to have a considerable effect on the liquid dynamics.

Here we study the dynamics of solvation water in the solvation sphere of organic and biological solutes by using solutes that are (for various reasons) “invisible” in the relevant frequency range. This allows us to subtract off the bulk water spectrum to yield the gigahertz to terahertz spectrum of pure solvation water for the first time.

Water Spectrum. The bulk water spectrum in the gigahertz–terahertz frequency range has three main peaks.^{5,9,10,19,20} Relatively sharp peaks at 1.1 and 4.5 THz correspond to the transverse (TA) and longitudinal (LA) acoustic phonon bands of water or alternatively the hydrogen-bond bend and stretch modes.⁹ The lowest frequency band, peaking at 250 GHz at room temperature and falling off smoothly to zero below 50 GHz, derives its intensity from collision-induced effects and is caused by translational rattling and diffusion. It is this translational band that will be the main reporter in this study.¹⁸ In liquids, one would normally expect to observe a band at a lower frequency due to orientational diffusion. However, because the molecular polarizability tensor of water is very nearly isotropic,²¹ this band is not seen in the anisotropic Raman spectrum of water.

Trimethylamine N-oxide. The first solute molecule to be investigated is trimethylamine N-oxide (TMAO, see the [SI](#)), which is amphiphilic and has been widely studied using Raman spectroscopy,^{22,23} THz-TDS,²⁴ dielectric spectroscopy,²⁵ and time-domain IR spectroscopy.^{26–28} TMAO is readily soluble in water. In our experiments, on increasing the concentration of

Received: May 8, 2017

Accepted: June 13, 2017

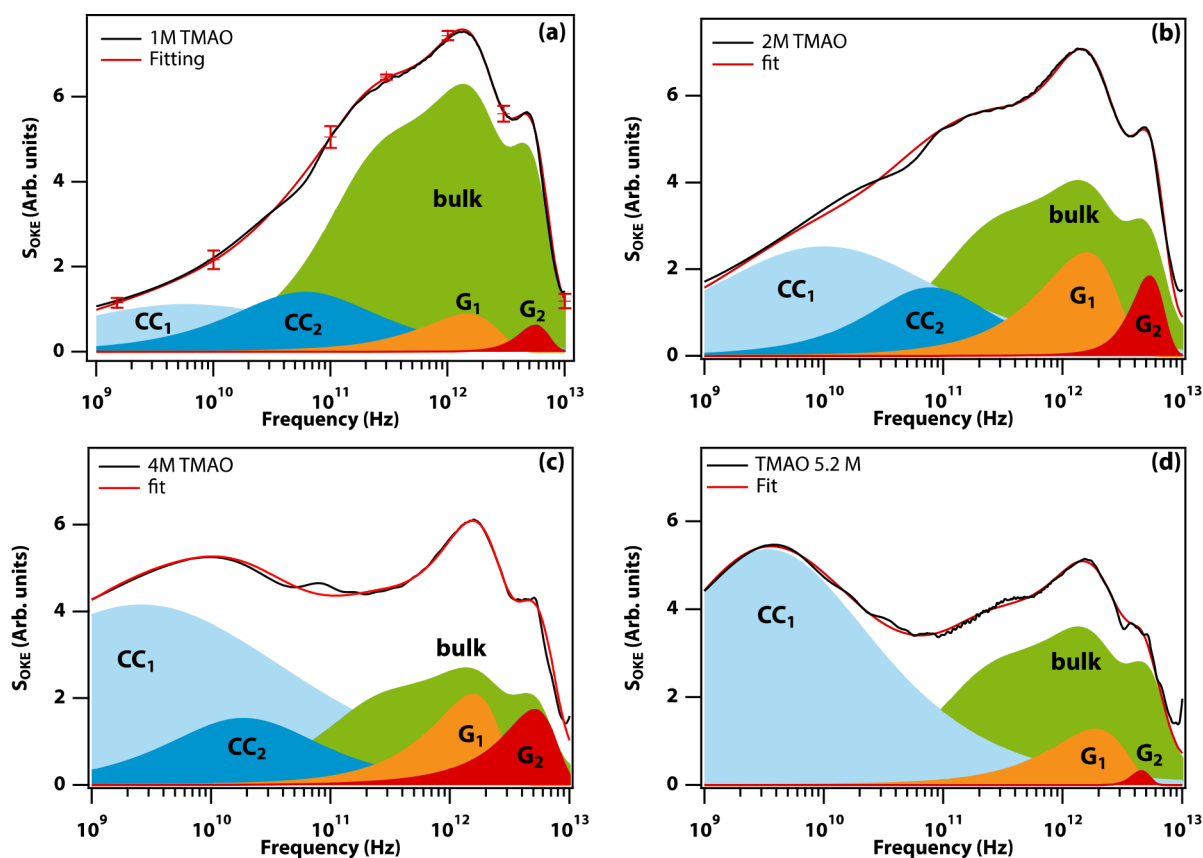


Figure 1. OKE spectra of aqueous solutions of TMAO. Raw OKE spectra of aqueous TMAO solutions at 1, 2, and 4 M and saturation (~ 5.2 M) at room temperature. Also shown are the results of a fitting procedure, as discussed in the text. CC: Cole–Cole function; G: Gaussian function; bulk: a separately determined³ spectrum of bulk water. The panel for 1 M TMAO also shows the estimated frequency-dependent error bars (see the SI).

TMAO in water, the OKE spectrum develops a new band in the 1–100 GHz region, while the spectrum remains largely unaltered in the terahertz frequency range. The raw OKE spectrum of a 1 M TMAO solution is shown in Figure 1a. Clearly, a major component of the solution spectrum is the spectrum of unaltered bulk water with additional amplitude in the gigahertz range (significantly larger than the estimated experimental error in this range).

In previous work,^{22,23} the gigahertz-frequency band was assigned to orientational diffusion of the TMAO molecule in its aqueous environment. Here we will show that this cannot be the case. The OKE (or reduced depolarized Raman) spectra of all anisotropically polarizable molecular liquids have the same generic form:^{15,29,30} a low-frequency orientational-diffusion band (α relaxation) below ~ 100 GHz (dependent on temperature and viscosity), intermediate-frequency modes due to translational motions (β relaxation), and one or more librational bands in the low terahertz frequency range. The orientational-diffusion band and librational band are always of the same magnitude as both are determined by the molecular anisotropic polarizability tensor.

Thus if the additional amplitude in the gigahertz range is caused by the orientational diffusion of TMAO, then one must also observe an equally strong contribution from TMAO librations in the terahertz range. As can be seen in Figure 1, the terahertz spectrum is essentially unaltered in shape, ruling out a new contribution from TMAO librations.

To confirm this, the OKE spectrum of TMAO in formamide was collected (see Figure 2). Again, no changes (except for

amplitude) are observed in the terahertz frequency part of the spectrum, where one would expect the librational band of TMAO to be present. Formamide has two librational bands at 3.3 and 5.7 THz,³¹ which are essentially unchanged in the TMAO solution. Changes seen in the gigahertz part of the spectrum are solely due to a shift of the orientational-diffusion band of formamide to lower frequencies, while the orientational-diffusion band of TMAO, which is expected to peak at 1.7 GHz (see the SI), is absent in the spectrum (but might be more difficult to detect due to congestion). The amplitude of the entire formamide spectrum is reduced, as expected, due to reduction of the formamide concentration on adding TMAO.

An OKE spectrum taken in molten TMAO dihydrate (8.8 M, 130 °C; see the SI) shows a shape characteristic of very high concentration aqueous solutions,^{32,33} with the 4.5 THz LA band strongly reduced leaving only the 1.1 THz TA band and the lower frequency translational band of “bulk” water. This measurement provides an upper estimate of the contribution of TMAO to the 1 M spectrum in Figure 1a of 0.05.

Thus the experimental data demonstrate that TMAO does not give rise to a detectable OKE signal and that all spectral changes are solely caused by the modification of the water dynamics induced by the presence of TMAO. A DFT calculation with a B3LYP/6-311++G(2df,p) level of theory with a continuum dielectric model for water was carried out to calculate the molecular polarizability tensor of TMAO (see the SI). This confirms that the anisotropic part is very small, consistent with the experimental results.

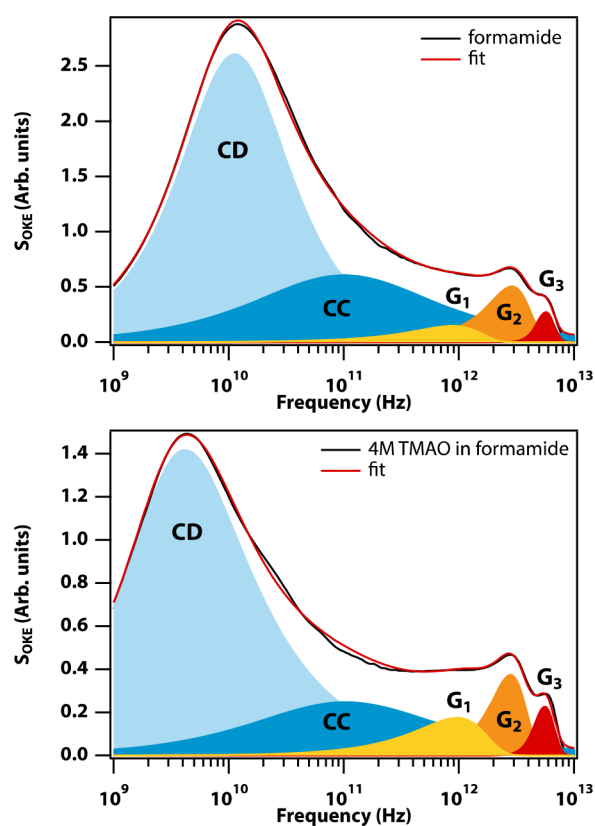


Figure 2. OKE spectra of formamide and a solution of TMAO in formamide. Raw OKE spectra of (top) formamide and (bottom) a 4-M solution of TMAO in formamide. Also shown are the results of a fitting procedure as discussed in the text. CD: Cole–Davidson function.

A TMAO in water orientational-diffusion band (if it were present) would be expected to follow a Debye function with a peak at 5.4 GHz based on a Stokes–Einstein–Debye calculation or 8.0 GHz based on a measurement using dielectric relaxation spectroscopy.²⁶ Instead, it is found that the new band is exceedingly broad (from ~ 1 to ~ 100 GHz) even at low concentrations where a large degree of inhomogeneity is not expected. Thus this result is also inconsistent with an assignment as an orientational-diffusion band, as previously reported.²²

Finally, one may consider the possibility that water molecules are strongly attached to TMAO in the first solvation shell and “ride” along with the reorientations of the solute while giving rise to an OKE signal. In that case, the effective hydrodynamic radius of the solute would increase. In the extreme case of a full water hydration shell riding along, the orientational diffusion band is expected to peak at 470 MHz (see the SI). Even a partial shell of water molecules riding along would give rise to a significant slowdown of the orientational dynamics and therefore cannot be a significant cause of additional intensity in the OKE spectrum in the 1–100 GHz range.

Thus it is confirmed that the aqueous TMAO solution spectrum has significant contributions only from bulk water and solvation water. The bulk-water contribution is estimated by fitting the data to a function representing the entire bulk-water spectrum,³ with only the amplitude as a free fit parameter. The solvation-water component is modeled using two Gaussian functions (see eq S4) representing the TA and LA phonon bands altered by the solute and two Cole–Cole functions (see

eq S2) representing the altered interaction-induced translational band. The solvation-water spectrum can then be extracted by taking this fit and setting the amplitude of the bulk-water component to zero (see Figure 3).

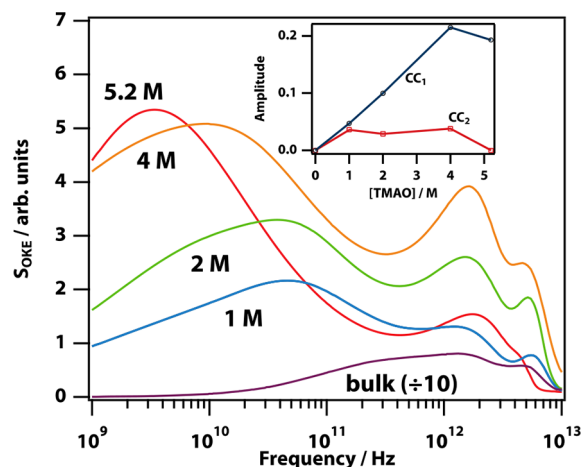


Figure 3. Comparison of the modified solvation-water spectra for different concentrations of TMAO. Bulk-water spectrum³ and concentration-dependent solvation-water spectra in aqueous TMAO solutions determined by a fitting procedure (see text) and leaving out the bulk-water contribution. (inset) The amplitude of the Cole–Cole functions representing super-slow (CC_1) and slow (CC_2) water components as a function of TMAO concentration (see Methods in the SI for details of fits).

A concentration-dependent study was carried out in aqueous TMAO solutions at 1, 2, and 4 M and saturation (~ 5.2 M) at room temperature (see Figure 1). Details of the fit parameters of the OKE spectra of all concentrations are provided in Tables S1–S4. At all concentrations, the solvation water LA and TA phonon bands are slightly blue-shifted compared with the bulk. The altered translational diffusion band in the gigahertz region increases in amplitude in proportion to the TMAO concentration. The two Cole–Cole bands clearly visible in Figure 1 represent populations of slow and super-slow water.

Figure 3 shows the solvation-water OKE spectra as a function of TMAO concentration as well as the bulk water spectrum at 25 °C. It can be seen that as the TMAO concentration increases, the low-frequency part of the spectrum shows a shift toward the lower frequency side. The ratio of the amplitudes of the translational diffusion of water and the phonon modes is very nearly constant until it increases at 4 M and dramatically so at 5.2 M. The inset of Figure 3 shows a plot of the amplitude of each Cole–Cole function representing slow and super-slow water content as a function of TMAO concentration. As the concentration of TMAO increases, the two water components respond differently; the super-slow component shows a steady increase, whereas the slow component saturates above ~ 1 M.

Polyhydroxylated Fullerene. Further experiments were carried out using other solutes in aqueous solution (see Figure 4) to check the generality of the effect. Buckminsterfullerene has icosahedral symmetry and is therefore expected not to give rise to an OKE signal in the low-frequency range. However, it is insoluble in water. Therefore, water-soluble polyhydroxylated fullerene (PHF), was used, which has a radius of 0.5 nm in water³⁴ while closely maintaining the high symmetry of buckminsterfullerene. Experiments were carried out on aqueous PHF solutions of 50 mg/mL (the approximate room-

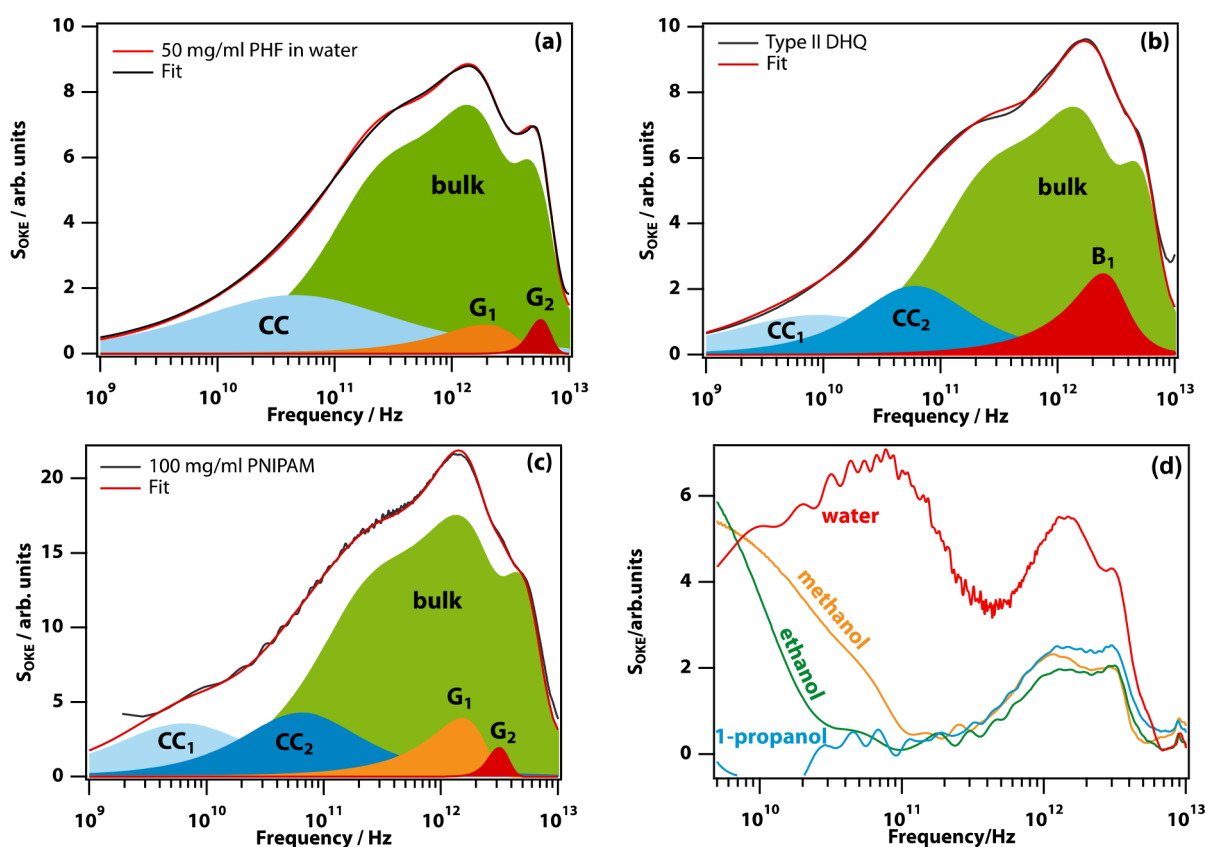


Figure 4. OKE spectra of additional solutions showing the perturbation of the solvation-shell dynamics. (a) Aqueous solution of 50 mg/mL polyhydroxylated fullerene (PHF). (b) Aqueous solution of the protein type II dehydroquinase (DHQ). (c) Aqueous solution of poly(*N*-isopropylacrylamide) (PNIPAm). (d) PNIPAm in different alcohol solutions: 100 mg/mL PNIPAm in water and 200 mg/mL in methanol, ethanol, and 1-propanol. Also shown in panels a–c are the results of a fitting procedure, as discussed in the text.

temperature solubility limit), resulting in a clear light-yellow solution.

As can be seen in Figure 4a, the OKE spectrum of aqueous PHF solution is very similar to that of TMAO with contributions from bulk and solvation water. Again, a solvation-water band due to slowed translational motions is seen, which can be fitted confidently with a single Cole–Cole function (see eq S2 in the Methods in the SI) peaking at 40 GHz with $\alpha = 0.668$, indicating a very wide range of translational diffusion time scales.

To confirm that buckminsterfullerene does not contribute to the OKE spectrum in the gigahertz range, a measurement was carried out on a solution of PHF in methanol (see the SI). As in TMAO in formamide, no buckminsterfullerene librational or vibrational bands are seen in the 1–5 THz range, nor is there a diffusional band peaking at 40 GHz. On the low-frequency end of the spectrum (<40 GHz), one observes the tail of a band that is likely to be from slowed down methanol in the solvation shell of PHF.

Type II DHQ. Previous studies on the protein lysozyme using Raman, OKE, and neutron scattering^{13,35} have shown that the translational diffusion of water molecules in the solvation layer gives rise to broad band peaking at ~ 20 GHz. However, in lysozyme, this band is obscured by the tail of the protein orientational-diffusion band. Lysozyme is a relatively small protein (hydrodynamic radius 1.9 nm), causing the orientational diffusion to be relatively fast (peaking at ~ 25.5 MHz) and therefore overlapping with the solvation-water band.¹³

To be able to observe the solvation-water band unobscured, one simply needs to select a much bigger protein in which the orientational-diffusion band is shifted to much lower frequency. Hence, we selected the dodecamer protein type II dehydroquinase (DHQ) with a molecular weight of 200 kDa.³⁶ This protein is roughly spherical in shape with a hydrodynamic radius of ~ 5 nm. The orientational diffusion of this protein in water peaks at ~ 1 MHz (see the SI).

Figure 4b shows the OKE spectrum of ~ 150 mg/mL DHQ. Unlike TMAO and PHF, proteins such as DHQ will contribute to the terahertz OKE spectrum, which makes it more difficult to disentangle the contributions from the protein, bulk water, and solvation water in this range. Here we find that the data can be fitted using a bulk-water spectrum with an additional Brownian band peaking at 3 THz and two Cole–Cole functions in the gigahertz range. The 3 THz band is different from that previously observed in lysozyme¹³ and most likely represents a combination of changes in the LA and TA phonon bands of solvation water and delocalized phonon bands of the protein. The gigahertz part of the spectrum again represents slowed translational motions in the solvation shell of DHQ possibly contaminated by structural relaxation and localized secondary relaxations of the protein.^{35,37} This broad feature is fitted with two Cole–Cole functions, which represent slow and super-slow distributions, as in the case of TMAO.

*Poly(*N*-isopropylacrylamide).* Proteins at desired concentrations for our experiments cannot typically be dissolved in solvents other than water. Therefore, it was decided to investigate poly(*N*-isopropylacrylamide) (PNIPAm), which is

Table 1. Slow-Down Factors Calculated for the Case of Different Solutes^a

	1 M TMAO	2 M TMAO	4 M TMAO	sat. TMAO	PHF	DHQ	PNIPAm
slow	4	4	10		6	4	4
super-slow	48	27	97	72		27	39

^aSlowdown of the translational water dynamics is calculated by taking the ratio of the time constant of each slow water component to the translational diffusion time constant of bulk water at 25 °C (0.649 ps).³

a thermosensitive water-soluble polymer that has many similarities to (unfolded) proteins taking on a random-coil conformation below 32 °C, resulting in a clear colorless solution.

The OKE spectrum of an aqueous solution of PNIPAm (Figure 4c) is again very similar, consisting of a large bulk-water component and slowed translational solvent–water contributions in the gigahertz range that can be fitted with two Cole–Cole functions. In the terahertz region, two modes at 1.5 and 3.1 THz are observed that fit well to antisymmetrized Gaussian functions, suggesting that these are shifted LA and TA phonon bands of solvation water.

Experiments were carried out on PNIPAm dissolved in methanol, ethanol, and 1-propanol (Figure 4d; see also the SI for comparisons with solvent spectra). Changing the solvent introduces many subtle changes in the terahertz frequency region, which are attributed to changes in terahertz frequency solvent modes as well as a component from PNIPAm itself. The orientational-diffusion band of PNIPAm is expected to be at very low frequencies due to the random-coil fold of the polymer. The experiments show considerable changes between water and the alcohols as solvents in the gigahertz range, ruling out an origin of these signals in side-chain motion, structural relaxation, or beta relaxations of the solute.

We have shown that TMAO and PHF do not contribute to the OKE (depolarized Raman) spectra, and this has allowed us to study solvation water directly without obstruction by the solutes. The protein DHQ is very large, and its orientational-diffusion band is expected to peak at ~1 MHz; therefore, one can exclude any protein orientational-diffusion contribution in the gigahertz range, while neutron scattering studies³⁵ have demonstrated that the gigahertz band originates in water. Similarly, PNIPAm solutions at the concentrations used are a gel, pushing the orientational diffusion band toward zero frequency, while experiments with different solvents rule out that the gigahertz band is caused by the motion of the polymer itself. Unfortunately, in the case of both DHQ and PNIPAm, the solutes make significant contributions to the terahertz part of the OKE spectrum.

Thus, in these widely different samples, we can isolate the OKE spectrum of solvated water. It is found that in all cases the LA and TA phonon bands are only mildly perturbed, while the solvation-water translational band is shifted to lower frequencies. The slowed down solvation-water band can be fitted to one or two Cole–Cole functions. For all cases, the super-slow component has a relatively low value of α (~0.6) compared with the slow component and therefore a wider frequency distribution. The slow component has a value of α comparable to the value (0.96) of the translational diffusion of bulk water.³

In the case of TMAO, as the concentration increases, the super-slow component takes the upper hand. In the saturated solution, only a wide super-slow component was observed. The structure of the water network in the solvation shell appears to become disrupted in the higher concentration TMAO

solutions, as indicated by the decreasing amplitude of the high-frequency LA phonon mode of water and the increased ratio of the amplitude of the translational diffusion band and the phonon bands (see Figure 3).

At higher concentrations, the solvation shell of each solute may be shared by nearby solutes, further slowing down the dynamics (see the SI). Previous experiments with salt solutions have shown that the translational diffusion of water molecules is slowed down, eventually leading to a complete arrest at a critical concentration.¹⁸ In the examples studied here, however, the slowdown is very significant, even at relatively low concentrations ranging from a factor of ~4 for the slow band to a factor of 27 to 48 for the superslow band (see Table 1). The translational-relaxation time constant for the superslow band (averaged over all five measured concentrations) is 37 ± 14 ps, which is slower than the predicted (29 ps) and measured (20 ps) orientational relaxation time of TMAO in water. This suggests that the superslow band is associated with water molecules in a solvation shell that is shared by two or more solutes.³⁸

Because the translational dynamics are slowed down by factors of 4 and more, the implication is that water molecules remain in the solvation shell of the solute for longer. Thus some of the orientational diffusion dynamics of the solutes might be reflected in the dynamics of the water molecules in the solvation shell. This may well explain the lower value of α in the Cole–Cole function describing the superslow component. The only way to disentangle these translational and orientational contributions is through molecular-dynamics simulations. Because the molecular polarizability tensor of water is very nearly isotropic,²¹ the low-frequency OKE (and Raman) spectrum of water is entirely caused by collision-induced effects. Thus such simulations will have to incorporate collision-induced effects on the polarizability tensors of both solute and water.

The water jump model proposed by Laage and Hynes considers the water orientational diffusion as a result of the large amplitude angular jumps when the OH groups exchange H-bond acceptors.^{1,39} The topology of the solute molecule plays a role here, as it restricts the degrees of freedom for the water molecules in the first solvation shell. For an infinite planar solute surface, this slows down the orientational dynamics by a factor of 2, for low concentrations of the solute. Thus the slowdown factors of ~4 observed here in the slow band are at odds with this model as well as previous measurements using other techniques on proteins and small solutes.^{1,26} They are consistent with recent observation of very slow and extremely inhomogeneous water translational dynamics in the solvation shell of DNA.³

In conclusion, slowed down water translational dynamics are observed in the solvation shell of different solutes. Previously unobserved, the distribution of the slowdown of dynamics is made visible by measuring the low-frequency spectrum of solvated water, for the first time, using solutes that do not contribute to the spectrum.

■ ASSOCIATED CONTENT

● Supporting Information

The Supporting Information is available free of charge on the ACS Publications website at DOI: 10.1021/acs.jpcl.7b01127. Raw data for the figures in this work are available from DOI: 10.5525/gla.researchdata.424.

Methods, estimation of errors, OKE modeling, calculations, supplementary figures, and fit parameters. (PDF)

■ AUTHOR INFORMATION

Corresponding Author

*E-mail: klaas.wynne@glasgow.ac.uk.

ORCID

Mario González-Jiménez: 0000-0002-8853-0588

Klaas Wynne: 0000-0002-5305-5940

Author Contributions

The experiments and data analysis were carried out by G.R. and M.G.-J., sample preparation by G.R. and A.J.L., interpretation by G.R. and K.W., and writing of the manuscript by K.W. aided by G.R. and M.G.-J.

Notes

The authors declare no competing financial interest.

■ ACKNOWLEDGMENTS

We thank the Engineering and Physical Sciences Research Council (EPSRC) for support through grants EP/J009733/1, EP/J00975X/1, EP/K034995/1, and EP/N508792/1.

■ REFERENCES

- (1) Fogarty, A. C.; Duboué-Dijon, E.; Sterpone, F.; Hynes, J.; Laage, D. Biomolecular Hydration Dynamics: A Jump Model Perspective. *Chem. Soc. Rev.* **2013**, *42* (13), 5672–5683.
- (2) Duboué-Dijon, E.; Fogarty, A. C.; Hynes, J.; Laage, D. Dynamical Disorder in the DNA Hydration Shell. *J. Am. Chem. Soc.* **2016**, *138* (24), 7610–7620.
- (3) González Jiménez, M.; Ramakrishnan, G.; Harwood, T.; Laphorn, A. J.; Kelly, S. M.; Ellis, E. M.; Wynne, K. Observation of Coherent Delocalized Phonon-Like Modes in DNA under Physiological Conditions. *Nat. Commun.* **2016**, *7*, 11799.
- (4) Hithell, G.; Gonzalez, M.; Greetham, G. M.; Donaldson, P. M.; Towrie, M.; Parker, A. W.; Burley, G. A.; Wynne, K.; Hunt, N. T. Ultrafast 2d-Ir and Optical Kerr Effect Spectroscopy Reveal the Impact of Duplex Melting on the Structural Dynamics of DNA. *Phys. Chem. Chem. Phys.* **2017**, *19* (16), 10333–10342.
- (5) Fukasawa, T.; Sato, T.; Watanabe, J.; Hama, Y.; Kunz, W.; Buchner, R. Relation between Dielectric and Low-Frequency Raman Spectra of Hydrogen-Bond Liquids. *Phys. Rev. Lett.* **2005**, *95* (19), 197802.
- (6) Popov, I.; Ishai, P. B.; Khamzin, A.; Feldman, Y. The Mechanism of the Dielectric Relaxation in Water. *Phys. Chem. Chem. Phys.* **2016**, *18* (20), 13941–13953.
- (7) Hansen, J. S.; Kisliuk, A.; Sokolov, A. P.; Gainaru, C. Identification of Structural Relaxation in the Dielectric Response of Water. *Phys. Rev. Lett.* **2016**, *116* (23), 237601–5.
- (8) Ronne, C.; Astrand, P.; Keiding, S. Thz Spectroscopy of Liquid H₂O and D₂O. *Phys. Rev. Lett.* **1999**, *82* (14), 2888–2891.
- (9) Walrafen, G. E. Raman-Spectrum of Water - Transverse and Longitudinal Acoustic Modes Below Almost-Equal-to 300 Cm⁻¹ and Optic Modes above Almost-Equal-to 300 Cm⁻¹. *J. Phys. Chem.* **1990**, *94* (6), 2237–2239.
- (10) Taschin, A.; Bartolini, P.; Eramo, R.; Righini, R.; Torre, R. Evidence of Two Distinct Local Structures of Water from Ambient to Supercooled Conditions. *Nat. Commun.* **2013**, *4*, 2401.
- (11) Turton, D. A.; Corsaro, C.; Martin, D. F.; Mallamace, F.; Wynne, K. The Dynamic Crossover in Water Does Not Require Bulk Water. *Phys. Chem. Chem. Phys.* **2012**, *14* (22), 8067–8073.
- (12) Xu, Y.; Havenith, M. Perspective: Watching Low-Frequency Vibrations of Water in Biomolecular Recognition by Thz Spectroscopy. *J. Chem. Phys.* **2015**, *143* (17), 170901–8.
- (13) Turton, D. A.; Senn, H. M.; Harwood, T.; Laphorn, A. J.; Ellis, E. M.; Wynne, K. Terahertz Underdamped Vibrational Motion Governs Protein-Ligand Binding in Solution. *Nat. Commun.* **2014**, *5*, 3999.
- (14) Meister, K.; Ebbinghaus, S.; Xu, Y.; Duman, J. G.; DeVries, A.; Gruebele, M.; Leitner, D. M.; Havenith, M. Long-Range Protein-Water Dynamics in Hyperactive Insect Antifreeze Proteins. *Proc. Natl. Acad. Sci. U. S. A.* **2013**, *110* (5), 1617–1622.
- (15) Turton, D. A.; Martin, D. F.; Wynne, K. Optical Kerr-Effect Study of Trans- and Cis-1,2-Dichloroethene: Liquid-Liquid Transition or Super-Arrhenius Relaxation. *Phys. Chem. Chem. Phys.* **2010**, *12* (16), 4191–4200.
- (16) Fecko, C.; Eaves, J.; Tokmakoff, A. Isotropic and Anisotropic Raman Scattering from Molecular Liquids Measured by Spatially Masked Optical Kerr Effect Spectroscopy. *J. Chem. Phys.* **2002**, *117* (3), 1139–1154.
- (17) Turton, D. A.; Wynne, K. Universal Nonexponential Relaxation: Complex Dynamics in Simple Liquids. *J. Chem. Phys.* **2009**, *131* (20), 201101.
- (18) Turton, D. A.; Hunger, J.; Hefter, G.; Buchner, R.; Wynne, K. Glasslike Behavior in Aqueous Electrolyte Solutions. *J. Chem. Phys.* **2008**, *128* (16), 161102.
- (19) Castner, E.; Chang, Y. J.; Chu, Y.; Walrafen, G. E. The Intermolecular Dynamics of Liquid Water. *J. Chem. Phys.* **1995**, *102* (2), 653–659.
- (20) Palese, S.; Mukamel, S.; Miller, R. J. D.; Lotshaw, W. Interrogation of Vibrational Structure and Line Broadening of Liquid Water by Raman-Induced Kerr Effect Measurements within the Multimode Brownian Oscillator Model. *J. Phys. Chem.* **1996**, *100* (24), 10380–10388.
- (21) Murphy, W. Rayleigh Depolarization Ratio and Rotational Raman-Spectrum of Water-Vapor and Polarizability Components for Water Molecule. *J. Chem. Phys.* **1977**, *67* (12), 5877–5882.
- (22) Comez, L.; Paolantoni, M.; Corezzi, S.; Lupi, L.; Sassi, P.; Morresi, A.; Fioretto, D. Aqueous Solvation of Amphiphilic Molecules by Extended Depolarized Light Scattering: The Case of Trimethylamine-N-Oxide. *Phys. Chem. Chem. Phys.* **2016**, *18* (13), 8881–8889.
- (23) Mazur, K.; Heisler, I. A.; Meech, S. R. Aqueous Solvation of Amphiphilic Solutes: Concentration and Temperature Dependent Study of the Ultrafast Polarizability Relaxation Dynamics. *Phys. Chem. Chem. Phys.* **2012**, *14* (18), 6343–6351.
- (24) Knake, L.; Schwaab, G.; Kartaschew, K.; Havenith, M. Solvation Dynamics of Trimethylamine N-Oxide in Aqueous Solution Probed by Terahertz Spectroscopy. *J. Phys. Chem. B* **2015**, *119* (43), 13842–13851.
- (25) Hunger, J.; Ottosson, N.; Mazur, K.; Bonn, M.; Bakker, H. J. Water-Mediated Interactions between Trimethylamine-N-Oxide and Urea. *Phys. Chem. Chem. Phys.* **2015**, *17* (1), 298–306.
- (26) Hunger, J.; Tielrooij, K.-J.; Buchner, R.; Bonn, M.; Bakker, H. J. Complex Formation in Aqueous Trimethylamine-N-Oxide (Tmao) Solutions. *J. Phys. Chem. B* **2012**, *116* (16), 4783–4795.
- (27) Bakulin, A. A.; Pshenichnikov, M. S.; Bakker, H. J.; Petersen, C. Hydrophobic Molecules Slow Down the Hydrogen-Bond Dynamics of Water. *J. Phys. Chem. A* **2011**, *115* (10), 1821–1829.
- (28) Rezus, Y. L. A.; Bakker, H. J. Observation of Immobilized Water Molecules around Hydrophobic Groups. *Phys. Rev. Lett.* **2007**, *99* (14), 148301.
- (29) Sonnleitner, T.; Turton, D. A.; Hefter, G.; Ortner, A.; Waselikowski, S.; Walther, M.; Wynne, K.; Buchner, R. Ultra-Broadband Dielectric and Optical Kerr-Effect Study of the Ionic Liquids Ethyl and Propylammonium Nitrate. *J. Phys. Chem. B* **2015**, *119* (29), 8826–8841.

(30) Turton, D. A.; Wynne, K. Stokes–Einstein–Debye Failure in Molecular Orientational Diffusion: Exception or Rule? *J. Phys. Chem. B* **2014**, *118* (17), 4600–4604.

(31) Faurskov Nielsen, O.; Lund, P. A.; Praestgaard, E. Hydrogen Bonding in Liquid Formamide. A Low Frequency Raman Study. *J. Chem. Phys.* **1982**, *77* (8), 3878–7.

(32) Amo, Y.; Tominaga, Y. Low-Frequency Raman Scattering of Koh and Naoh Aqueous Solutions. *J. Raman Spectrosc.* **2000**, *31* (7), 547–553.

(33) Amo, Y.; Tominaga, Y. Dynamical Structure of Water in Aqueous Solutions of LiCl, NaCl, and KCl by Low-Frequency Raman Scattering: Comparison between the Multiple Random Telegraph Model and Cole-Cole Relaxation. *Phys. Rev. E: Stat. Phys., Plasmas, Fluids, Relat. Interdiscip. Top.* **1998**, *58* (6), 7553–7560.

(34) Nakamura, Y.; Ueno, H.; Kokubo, K.; Ikuma, N.; Oshima, T. *J. Nanopart. Res.* **2013**, *15*, 1.

(35) Perticaroli, S.; Comez, L.; Paolantoni, M.; Sassi, P.; Lupi, L.; Fioretto, D.; Paciaroni, A.; Morresi, A. Broadband Depolarized Light Scattering Study of Diluted Protein Aqueous Solutions. *J. Phys. Chem. B* **2010**, *114* (24), 8262–8269.

(36) Roszak, A. W.; Robinson, D. A.; Krell, T.; Hunter, I. S.; Fredrickson, M.; Abell, C.; Coggins, J. R.; Laphorn, A. J. The Structure and Mechanism of the Type II Dehydroquinase from *Streptomyces Coelicolor*. *Structure* **2002**, *10* (4), 493.

(37) Khodadadi, S.; Sokolov, A. P. Protein Dynamics: From Rattling in a Cage to Structural Relaxation. *Soft Matter* **2015**, *11* (25), 4984–4998.

(38) Stirnemann, G.; Sterpone, F.; Laage, D. Dynamics of Water in Concentrated Solutions of Amphiphiles: Key Roles of Local Structure and Aggregation. *J. Phys. Chem. B* **2011**, *115* (12), 3254–3262.

(39) Laage, D. A Molecular Jump Mechanism of Water Reorientation. *Science* **2006**, *311* (5762), 832–835.